



## Young's Type Interference for Probing the Mode Symmetry in Photonic Structures

F. Intonti,<sup>1,2,\*</sup> F. Riboli,<sup>1</sup> N. Caselli,<sup>1</sup> M. Abbarchi,<sup>1</sup> S. Vignolini,<sup>1</sup> D. S. Wiersma,<sup>1,3</sup> A. Vinattieri,<sup>1,2</sup> D. Gerace,<sup>4</sup> L. Balet,<sup>5,6,†</sup> L. H. Li,<sup>5,‡</sup> M. Francardi,<sup>7</sup> A. Gerardino,<sup>7</sup> A. Fiore,<sup>6</sup> and M. Gurioli<sup>1,2</sup>

<sup>1</sup>European Laboratory for Non-linear Spectroscopy, 50019 Sesto Fiorentino (FI), Italy

<sup>2</sup>Università di Firenze, Dipartimento di Fisica e Astronomia, 50019 Sesto Fiorentino (FI), Italy

<sup>3</sup>National Institute for Optics (CNR-INO), 50019 Sesto Fiorentino (FI), Italy

<sup>4</sup>Dipartimento di Fisica "A. Volta", Università di Pavia, via Bassi 6, 27100 Pavia, Italy

<sup>5</sup>IPQE, Ecole Polytechnique Federale de Lausanne, CH-1015 Lausanne, Switzerland

<sup>6</sup>COBRA Research Institute, Eindhoven University of Technology, 5600 MB Eindhoven, The Netherlands

<sup>7</sup>Institute of Photonics and Nanotechnology, CNR, 00156 Roma, Italy

(Received 5 August 2010; revised manuscript received 11 February 2011; published 8 April 2011)

A revisited realization of the Young's double slit experiment is introduced to directly probe the photonic mode symmetry by photoluminescence experiments. We experimentally measure the far field angular emission pattern of quantum dots embedded in photonic molecules. The experimental data well agree with predictions from Young's interference and numerical simulations. Moreover, the vectorial nature of photonic eigenmodes results in a rather complicated parity property for different polarizations, a feature which has no counterpart in quantum mechanics.

DOI: 10.1103/PhysRevLett.106.143901

PACS numbers: 42.25.Hz, 42.50.Pq, 42.70.Qs

The Young's double slit experiment has been used for probing the wave nature of many different systems, such as light, sound, electrons, atoms and molecules. The original realization consists in a monochromatic light which illuminates, with the same phase in the near field (NF), two nearby slits and the diffracted light interferes in the far field (FF), demonstrating the wave character of light more than 200 years ago. Historically, Young's interference has then played a fundamental role in the understanding the wave and particle duality of matter in quantum mechanics. [1] Recently it has been successfully revisited in plasmonics [2], attosecond [3], molecular physics [4] and nonlinear optics [5].

Here we propose a revisited photonic Young's like experiment, where the slits are replaced by two identical photonic structures with embedded quantum emitters (i.e., quantum dots). In particular we use coupled photonic crystal microcavities (MCs) (see Fig. 1) often denominated as photonic crystal molecules [6–8]. These systems have been proposed for novel photonic devices [9] and for application in quantum information and communication [10,11]. Similar to the case of electronic states, both homo-atomic and hetero-atomic photonic molecules have been recently realized [12]. By exploiting NF mapping of the photonic eigenstates [13,14], the transition from localized to delocalized modes as a function of the mode detuning has been lately demonstrated [8,15]. Still the symmetry of the coupled modes is more difficult to be tested, as it refers to a phase property of the modes. Recently, phase sensitive techniques have been developed both in the NF [16] and in the FF [17], by interferometric methods and resonant elastic scattering. We demonstrate that Young's type interference can be used to directly probe

the photonic mode symmetry by simply using FF photoluminescence analysis.

In an ideal photonic molecule, the mode coupling results in a frequency splitting of the eigenvalues and in the formation of delocalized symmetric (with "+" sign) and antisymmetric (with "-" sign) eigenvectors, with an electric field described by

$$\mathbf{E}_{\pm}(\mathbf{r}) = \mathbf{E}_0(\mathbf{r} - \mathbf{d}) \pm \mathbf{E}_0(\mathbf{r} + \mathbf{d}), \quad (1)$$

where  $\mathbf{E}_0(\mathbf{r})$  represents the electric field mode of the single MC centered at  $\mathbf{r} = 0$  and  $2\mathbf{d}$  is the spatial separation between the two MCs. Note that there is a strict similarity of Eq. (1) with the orbitals of the  $\text{H}_2^+$  molecule, nevertheless, the photonic orbitals are vectorial.

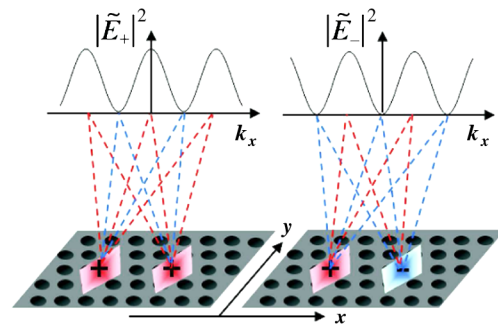


FIG. 1 (color online). Scheme of the emission patterns of two coupled modes  $\mathbf{E}_+(\mathbf{r})$  (left) and  $\mathbf{E}_-(\mathbf{r})$  (right) in a photonic microcavity molecule. The rhombs indicate the electric field distributions of the two modes, with a color scale to emphasize the positive (red) and negative (blue) amplitude. Red (blue) dashed lines indicate the constructive (destructive) optical paths in the far field emission patterns.

The mode  $\mathbf{E}_+(\mathbf{r})$  arises from two in phase single cavity modes and we expect to observe constructive interference along the normal direction, (as in the original Young's double slits experiment). The mode  $\mathbf{E}_-(\mathbf{r})$  arises from two out of phase single cavity modes and we expect to find destructive interference along the normal direction (see Fig. 1). This can be formally expressed by considering the Fourier transform of Eq. (1). After straightforward calculations, we have:

$$\tilde{\mathbf{E}}_+(\mathbf{k}) = 2\tilde{\mathbf{E}}_0(\mathbf{k}) \cos(\mathbf{k} \cdot \mathbf{d}) \quad (2)$$

$$\tilde{\mathbf{E}}_-(\mathbf{k}) = 2i\tilde{\mathbf{E}}_0(\mathbf{k}) \sin(\mathbf{k} \cdot \mathbf{d}) \quad (3)$$

where  $\tilde{\mathbf{E}}_n(\mathbf{k})$  is the spatial Fourier transform of  $\mathbf{E}_n(\mathbf{r})$  (with  $n = +, -, 0$ ). Therefore the symmetry of the coupled modes has a very strong impact on their angular emission pattern. We will use these equations for building up the FF patterns of the coupled modes by using the numerically simulated FF patterns of the modes of the single cavity. These FF patterns, reported in the figures with a red frame, will be denominated as Young's predictions in the following.

The investigated sample consists in a 320 nm-thick GaAs membrane with three layers of high-density InAs QDs emitting at 1300 nm grown by molecular beam epitaxy at the center of the membrane [18]. The photonic structure is a two dimensional triangular lattice where the single cavity, denominated  $D2$ , is formed by four missing holes [see the scanning electron microscope (SEM) image Fig. 2(b)]. The photonic molecules are designed in two different configurations. Henceforth we will refer to vertically (horizontally) aligned  $D2$  cavities if the major (minor) diagonals of the two adjacent  $D2$  cavities lie along the same line (see the SEM images in Figs. 3 and 4). The MCs were characterized in a microphotoluminescence (PL) setup using a  $NA = 0.7$  microscopy objective. The external cone of view is then  $45^\circ$  with respect to the normal to the sample surface and the angular resolution is  $8^\circ$ . For excitation we used a solid-state laser emitting at 532 nm. PL emission from the sample was collected with the fiber, dispersed by a spectrometer and detected by a cooled InGaAs array; the spectral resolution is of the order of 0.1 nm. Finally, numerical calculations were performed with a finite-difference time domain (FDTD) solver package. In the following, we will use the labels  $M1$  and  $M2$  for the first two modes of the single  $D2$  cavity and the labels  $P1 - P4$  for the first four modes of the coupled  $D2$  cavities.

In order to exploit the effects of the Young's double slit interference described by Eqs. (2) and (3) to probe the mode symmetry of a photonic molecule, we need to measure the NF and FF patterns of the single cavity modes. The main properties of a single  $D2$  cavity are summarized in Fig. 2. The mode  $M1$  is mainly polarized along the  $x$  direction, while the mode  $M2$  is characterized by an

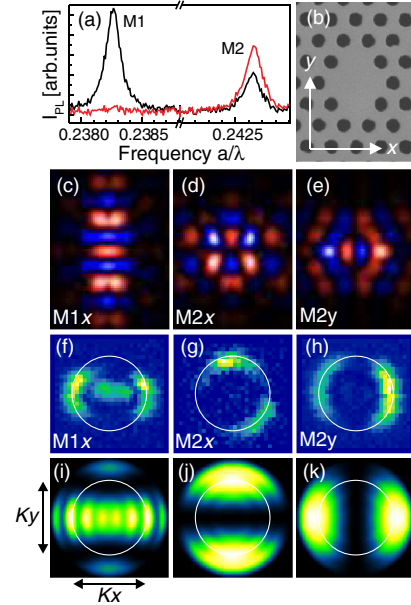


FIG. 2 (color online). Single  $D2$  cavity. (a) PL spectra in the  $x$  (black line) and  $y$  (red line) polarization channels. (b) SEM image. (c)–(e) Electric field FDTD NF maps: (c)  $x$  component of  $M1$ , (d)  $x$  component of  $M2$ , (e)  $y$  component of  $M2$ . (f)–(h) Experimental PL FF intensity  $k$  patterns: (f)  $x$  polarization of  $M1$ , (g)  $x$  polarization of  $M2$ , (h)  $y$  polarization of  $M2$ . (i)–(k) FDTD FF intensity  $k$  pattern: (i)  $x$  polarization of  $M1$ , (j)  $x$  polarization of  $M2$ , (k)  $y$  polarization of  $M2$ . SEM and NF images are  $1.5 \mu\text{m} \times 2.0 \mu\text{m}$ . In the NF maps red (blue) color indicates the positive (negative) amplitude. The FF patterns cover the whole external solid angle and the white circles are the experimental cone of view.

elliptical polarization [19]. Here and in the following, different scale colors are used for different maps. The NF maps show the electric field amplitude with a scale color to indicate the amplitude sign. The FF intensity  $k$  patterns are shown on blue (black) background for the PL experimental data (FDTD simulations). To describe synthetically the mode parity, we will use the denomination  $x$ -even ( $x$ -odd) for an even (odd) mode with respect to  $x$  inversion, etc. The FDTD NF maps of the significant electric field components are reported in Figs. 2(c)–2(e). The mode  $M1$  is elongated along the  $y$  direction and it is an  $x$ -even and  $y$ -even mode. The mode  $M2$  is more symmetrically distributed (with a slight elongation along  $x$ ) and the two polarizations have opposite parity. The  $x$  polarization is  $x$  even and  $y$  odd, while the  $y$  polarization is  $x$  odd and  $y$  even. As recently demonstrated FF measurements are a powerful tool for studying important aspects of photonics modes [20], as mode losses [21], role of disorder [22], etc. We found that the PL FF intensity  $k$  patterns are very different for the three cases.  $M1$  shows an horizontal stripe with a maximum at the center.  $M2$  shows a dark central region which is vertical and horizontal for the  $x$  and  $y$  polarizations, respectively. The experimental data nicely agree with the FDTD simulations. Obviously the FF  $k$

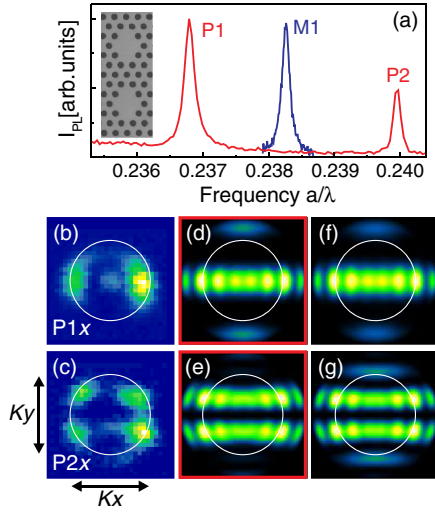


FIG. 3 (color online). Vertically aligned photonic molecule. (a) PL spectrum (red line) compared with the PL spectrum of the single  $D2$  MC (blue line), the inset shows the SEM image. (b) and (c) Experimental PL FF intensity  $k$  patterns of  $P1$  and  $P2$ . (d) and (e) Young's predictions of "+" and "-" modes. (f) and (g) FDTD FF intensity  $k$  patterns of  $P1$  and  $P2$ . The FF patterns cover the whole external solid angle and the white circles are the experimental cone of view.

patterns directly follow from the NF maps and two points help in understanding them. (i) Diffraction imposes that the FF pattern is elongated in the perpendicular direction with respect to the NF map (see  $M1$ ). (ii)  $x$ -odd ( $y$ -odd) modes destructively interfere in the FF along  $k_x = 0$  ( $k_y = 0$ ) (see the two polarizations of  $M2$ ).

As a consequence of the different NF elongation of  $M1$  and  $M2$ , we previously demonstrated that the photonic coupling is selective with respect to the geometrical configuration [8]. Therefore, in the case of vertical coupling, we limit our analysis to the  $P1$  and  $P2$  modes arising from the overlap of the two  $M1$  modes. Figure 3(a) shows the comparison of the PL spectra for the single  $D2$  cavity and the vertically aligned photonic molecule, in the inset a SEM image of the sample is displayed. In Figs. 3(b) and 3(c) we report the experimental PL FF  $k$  patterns of  $P1$  and  $P2$ , which turn out to be very different. Along the  $k_y = 0$  direction, we observe an enhancement of  $P1$  while the FF  $k$  pattern of  $P2$  shows a dark region. Figs. 3(d) and 3(e) show the Young's predictions (with red frames) for constructive [Eq. (2)] and destructive [Eq. (3)] interference, respectively. The comparison with the PL data clearly indicate that  $P1$  is the symmetric coupled mode and  $P2$  is the antisymmetric coupled mode. The FDTD simulations, shown in Figs. 3(f) and 3(g) agree well with the data and with the Young's predictions.

More complex, but also more interesting, is the case of the horizontally aligned  $D2$  photonic molecule, where, due to the selective coupling, we analyze the  $P3$  and  $P4$  modes arising from the overlap of the two  $M2$  modes of the single

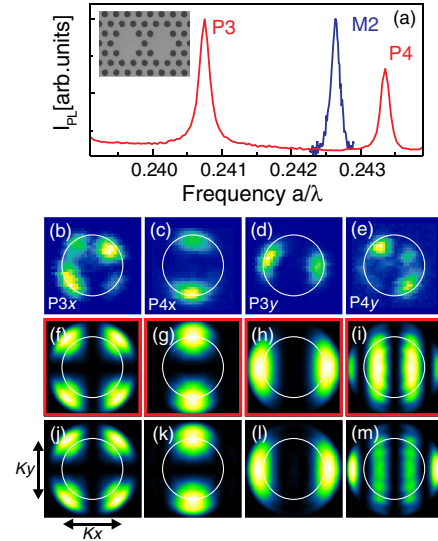


FIG. 4 (color online). Horizontally aligned photonic molecule. (a) PL spectrum (red line) compared with the PL spectrum of the single  $D2$  MC (blue line), the inset shows the SEM image. (b)–(e) Experimental PL FF intensity  $k$  patterns: (b) and (c)  $x$  polarization of  $P3$  and  $P4$ ; (d) and (e)  $y$  polarization of  $P3$  and  $P4$ . (f)–(i) Young's predictions: (f) and (g)  $x$  polarization of "-" and "+" modes; (h) and (i)  $y$  polarization of "-" and "+" modes. (j)–(m) FDTD FF intensity  $k$  patterns. (j) and (k)  $x$  polarization of  $P3$  and  $P4$ ; (l) and (m)  $y$  polarization of  $P3$  and  $P4$ . The FF patterns cover the whole external solid angle and the white circles are the experimental cone of view.

$D2$  cavity [8]. Figure 4(a) shows the comparison of the PL spectra between the single  $D2$  cavity and the horizontally aligned photonic molecule (the inset shows the SEM image). Because of the elliptical polarization of the  $M2$  mode, we need to study separately the FF patterns for the  $x$  and  $y$  polarizations.

In Figs. 4(b) and 4(c) we report the experimental PL FF  $k$  patterns of  $P3$  and  $P4$  for the  $x$  polarization. In Figs. 4(d) and 4(e) we report the experimental PL FF  $k$  patterns of  $P3$  and  $P4$  for the  $y$  polarization. All these patterns turn out to be very different. The comparison with the Young's predictions (with red frames in Fig. 4) helps in understanding them and assesses the mode symmetry. Note that for horizontally aligned cavities the Young's interference occurs along  $k_x = 0$ . The case of  $x$  polarization is simpler for recognizing the mode symmetry, since along  $k_x = 0$  the FF  $k$  pattern of the  $x$  polarization of  $M2$  has not zero intensity [see Fig. 2(j)]. In Fig. 4(c) we observe an enhancement along the  $k_x = 0$  direction for the FF  $k$  pattern of  $P4$ , while the FF  $k$  pattern of  $P3$  [see Fig. 4(b)] shows a dark region along the  $k_x = 0$  direction. We conclude that  $P3$  and  $P4$  are the antisymmetric and symmetric coupled modes, respectively. In the case of  $y$  polarization the understanding of the FF  $k$  patterns of  $P3$  and  $P4$  is more problematic. The fingerprint of destructive interference for  $P3$  is the broadening of the dark region along the

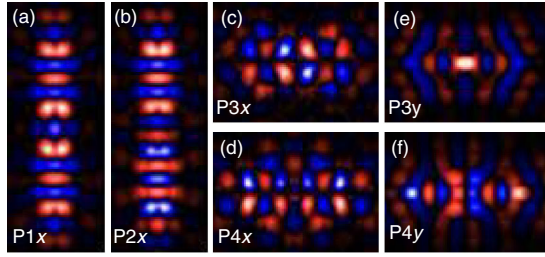


FIG. 5 (color online). Electric field FDTD NF maps for the coupled modes. The color scale indicates the positive (red) and negative (blue) amplitude; (a) and (b)  $x$  component of  $P1$  and  $P2$  for vertical coupling; the maps are  $1.4 \mu\text{m} \times 3.5 \mu\text{m}$ ; (c) and (d)  $x$  component of  $P3$  and  $P4$  for horizontal coupling; (e) and (f)  $y$  component of  $P3$  and  $P4$  for horizontal coupling; the maps are  $2.3 \mu\text{m} \times 1.7 \mu\text{m}$ .

$k_x = 0$  direction [see Fig. 4(d)]. The case of  $y$  polarization of  $P4$  is quite puzzling: one may expect to find a bright region along  $k_x = 0$  (due to Young’s like constructive interference), while a dark region is observed [see Fig. 4(e)]. This is because the FF  $k$  pattern of the  $y$  polarization of  $M2$  has zero intensity along the  $k_x = 0$  [see Fig. 2(k)]. The signature of the constructive interference for  $P4$  can be retrieved in the two additional vertical dark fringes around  $\pm 40^\circ$ , which correspond to the first zero of the Young’s modulation  $\cos(\mathbf{k} \cdot \mathbf{d})$  in Eq. (2). The FDTD simulations agree with the data and with the Young’s predictions, even if sizeable differences are found in the case of  $y$  polarization of  $P4$ . The origin of these discrepancies is related to the slight hybridization of the molecular modes. Indeed the NF pattern of  $P4y$  is not exactly reproduced by Eq. (1), if  $\mathbf{E}_0(\mathbf{r})$  is the  $y$  component of  $M2$ . Young predictions are indeed exact only in ideal molecules made by MC with one single mode.

Let us finally analyze the FDTD NF maps of the electric field amplitudes, which are reported in Fig. 5. As expected, it follows that  $P1$  and  $P2$  [see Figs. 5(a) and 5(b)], for vertical coupling, are  $y$ —even and  $y$ —odd, respectively. More complex is the case of  $P3$  and  $P4$  for horizontal coupling, where it is the  $x$ —symmetry which defines the Young interference. The  $P3$  mode is  $x$ —odd for the  $x$  polarization and  $x$ —even for the  $y$  polarization [see Figs. 5(c) and 5(d)]. The two polarizations of the  $P4$  mode have opposite  $x$ —parity with respect to  $P3$  [see Figs. 5(e) and 5(f)]. These puzzling parity properties of  $P3$  and  $P4$  can be understood by simply noting that the “symmetric” mode  $\mathbf{E}_+(\mathbf{r})$  is  $x$ —even ( $x$ —odd) whenever  $\mathbf{E}_0(\mathbf{r})$  is  $x$ —even ( $x$ —odd). On the contrary, the “antisymmetric” mode  $\mathbf{E}_-(\mathbf{r})$  is  $x$ —odd ( $x$ —even) whenever  $\mathbf{E}_0(\mathbf{r})$  is  $x$ —even ( $x$ —odd). Then, remembering the parity properties of  $M2$  (see Fig. 2), we conclude that the mode  $P3$  corresponds to the  $\mathbf{E}_-(\mathbf{r})$  and the  $P4$  mode corresponds

to the  $\mathbf{E}_+(\mathbf{r})$ . It follows that there may be a difference between parity (with respect to inversion) and symmetry (with respect to the mode building).

In conclusion, we have demonstrated that a revised Young’s double slit experiment can be used to probe the photonic mode symmetry. The constructive (destructive) FF interference is a direct signature of the symmetric (antisymmetric) mode property, arising from the electromagnetic coupling in a photonic crystal molecule. Moreover, the vectorial character of the photonic eigenmodes of the photonic crystal molecule results in a rather complicated parity property for different polarizations. This feature does not have a counterpart in the analogous quantum mechanical problem (i.e., the  $\mathbf{H}_2^+$  molecule). Young’s like photonic interference may open up interesting possibilities, controlling and matching the NF phases of two nearby quantum sources to implement novel devices for quantum information applications.

We thank Nicola Dotti for his help in the experimental setup. We acknowledge financial support from FAR (851) and PRIN (2008H9ZAZR003) projects.

\*intonti@lens.unifi.it

†Present address: CSEM SA, CH 2002 Neuchâtel, Switzerland.

‡Present address: The University of Leeds, Leeds LS2 9JT, United Kingdom.

- [1] C. J. Davissou and L. H. Germer, *Nature (London)* **119**, 558 (1927).
- [2] H. F. Schouten *et al.*, *Phys. Rev. Lett.* **94**, 053901 (2005).
- [3] F. Lindner *et al.*, *Phys. Rev. Lett.* **95**, 040401 (2005).
- [4] L. Ph. H. Schmidt *et al.*, *Phys. Rev. Lett.* **101**, 173202 (2008).
- [5] D. Gachet, S. Brustlein, and H. Rigneault, *Phys. Rev. Lett.* **104**, 213905 (2010).
- [6] M. Bayer *et al.*, *Phys. Rev. Lett.* **81**, 2582 (1998).
- [7] M. Benyoucef, S. Kiravittaya, Y. F. Mei, A. Rastelli, and O. G. Schmidt, *Phys. Rev. B* **77**, 035108 (2008).
- [8] S. Vignolini *et al.*, *Appl. Phys. Lett.* **94**, 151103 (2009).
- [9] T. Baba, *Nat. Photon.* **2**, 465 (2008).
- [10] D. Gerace *et al.*, *Nature Phys.* **5**, 281 (2009).
- [11] A. Dousse *et al.*, *Nature (London)* **466**, 217 (2010).
- [12] S. Vignolini *et al.*, *Appl. Phys. Lett.* **97**, 063101 (2010).
- [13] F. Intonti *et al.*, *Phys. Rev. B* **78**, 041401(R) (2008).
- [14] M. Burrese *et al.*, *Science* **326**, 550 (2009).
- [15] S. Vignolini *et al.*, *Appl. Phys. Lett.* **96**, 141114 (2010).
- [16] M. L. M. Balistreri *et al.*, *Science* **294**, 1080 (2001).
- [17] N. Le Thomas *et al.*, *Phys. Rev. B* **77**, 245323 (2008).
- [18] M. Francardi *et al.*, *Phys. Status Solidi C* **3**, 3693 (2006).
- [19] S. Vignolini *et al.*, *Appl. Phys. Lett.* **94**, 163102 (2009).
- [20] N. Le Thomas *et al.*, *J. Opt. Soc. Am. B* **24**, 2964 (2007).
- [21] J. Jagerska *et al.*, *Appl. Phys. Lett.* **95**, 111105 (2009).
- [22] N. Le Thomas *et al.*, *Phys. Rev. B* **79**, 033305 (2009).